processes

MDPI

Article

Glutathione Immobilized Polycaprolactone Nanofiber Mesh as a Dermal Drug Delivery Mechanism for Wound Healing in a Diabetic Patient

Morshed Khandaker [1,*], Niyaf Alkadhem [1], Helga Progri [1], Sadegh Nikfarjam [2], Jiyoon Jeon [3], Hari Kotturi [2] and Melville B. Vaughan [2]

[1] Department of Engineering & Physics, University of Central Oklahoma, Edmond, OK 73034, USA; biotechno.new.era@googlemail.com (N.A.); hprogri@uco.edu (H.P.)
[2] Department of Biology, University of Central Oklahoma, Edmond, OK 73034, USA; snikfarjam@uco.edu (S.N.); hkotturi@uco.edu (H.K.); mvaughan4@uco.edu (M.B.V.)
[3] Forensic Science Institute, University of Central Oklahoma, Edmond, OK 73034, USA; jjeon2@uco.edu
* Correspondence: mkhandaker@uco.edu; Tel.: +1-405-974-5935; Fax: +1-405-974-3812

Abstract: Glutathione (GSH) is an anti-inflammatory and antioxidant biomolecule. Polycaprolactone (PCL) nanofiber mesh (NFM) is capable of the attachment and release of biomolecules for prolonged periods and has the potential as a transdermal drug delivery system during wound healing for a diabetic patient. Our earlier study found that high levels of sugar in diabetic male mice were significantly decreased by daily doses of glutathione administered on the mice. Furthermore, oxidative stress found in diabetic male mice led to the total depletion of glutathione levels in the body's organs (pancreas, spleen, epididymis, and testis). The objective of this study was to attach GSH with PCL NFM for the controlled release of GSH biomolecules for long periods of time from the fiber mesh into a diabetic body. This study produced PCL NFM using an electrospun technique and tested it on mice to evaluate its efficiency as a dermal drug delivery mechanism. This study dissolved GSH (2.5 mg/mL) with phosphate-buffered saline (PBS) and glutaraldehyde (GLU) solution to create GSH-PBS and GSH-GLU complexes. Each complex was used to soak PCL NFM for 24 h and dried to create PCL-GSH-PBS and PCL-GSH-GLU meshes. Fiber morphology, degradation, fibroblast cell proliferation, cytotoxicity, and GSH release activities from each mesh were compared. Fibroblast cell adhesion and cytotoxicity tests found excellent biocompatibility of both GSH-immobilized PCL meshes and no degradation until 20 days of the study period. The disk diffusion method was conducted to test the antibacterial properties of the sample groups. Release tests confirmed that the attachment of GSH with PCL by GSH-GLU complex resulted in a steady release of GSH compared to the fast release of GSH from PCL-GSH-PBS mesh. The disk diffusion test confirmed that PCL-GSH-GLU has antibacterial properties. The above results conclude that GSH-GLU immobilized PCL NFM can be a suitable candidate for a transdermal anti-oxidative and anti-bacterial drug delivery system such as bandage, skin graft for wound healing application in a diabetic patient.

Keywords: glutathione; diabetic; polycaprolactone; nanofibers; drug delivery; antioxidant; anti-inflammatory

Citation: Khandaker, M.; Alkadhem, N.; Progri, H.; Nikfarjam, S.; Jeon, J.; Kotturi, H.; Vaughan, M.B. Glutathione Immobilized Polycaprolactone Nanofiber Mesh as a Dermal Drug Delivery Mechanism for Wound Healing in a Diabetic Patient. *Processes* **2022**, *10*, 512. https://doi.org/10.3390/pr10030512

Academic Editor: Angela Scala

Received: 28 December 2021
Accepted: 25 February 2022
Published: 4 March 2022

1. Introduction

Diabetics have high levels of reactive oxygen species (ROS) and not enough antioxidants to neutralize them [1]. Diabetics also have low levels of intracellular glutathione [2]. Enzymatic glutathione redox systems, such as glutathione (GSH), glutathione reductase (GR), and glutathione peroxidase (Gpx), can neutralize excess ROS and maintain a proper cellular environment [3]. Free radicals are formed disproportionately in diabetes; abnormally high levels of free radicals and the simultaneous decline of antioxidant defense mechanisms can lead to the development of insulin resistance [4]. These consequences of oxidative stress can promote the development of complications such as diabetes mellitus [5].

Concerning diabetes, antioxidant supplementation has shown benefits and is currently available in the market as oral medicine. GSH antioxidant therapy could alleviate the increased oxidative stress and emerge as an additional therapeutic modality as inflammation leads to insulin resistance and Type 2 diabetes [6]. Diabetic body organs have high levels of oxidative stress, which means too much free ROS and not enough antioxidants to neutralize them [1]. Oxidative stress plays a major role in the pathogenesis of bone in both types of diabetes mellitus. Researchers found that ROS participates in bone remodeling, with direct involvement of osteoclast-generated superoxide and bone degradation [7]. The enzymatic glutathione redox system has emerged as a supplementary therapeutic drug for diabetics to alleviate the increased presence of oxidative stress and inflammation. Several in vitro and animal studies have shown that oxidative stress diminishes bone formation by reducing the differentiation and survival of osteoblasts [8]. Clinical studies have also suggested that the involvement of antioxidants plays a role in the pathogenesis of bone and muscle loss [9]. However, according to the author's knowledge, a dermal antioxidant delivery mechanism for diabetic patients has not been explored yet. The goal of this study is to develop a mechanism for the delivery of GSH through a skin patch on a diabetic body.

Over the past three decades, there have been advances in skin regeneration using tissue engineering approaches [10]. However, there is no antibacterial bandage available in the market that is particularly suitable for a patient with diabetes. Diabetic patients are prone to microbial-induced inflammation due to diseases or skin injuries. Diabetic skin ulcers are not only painful diseases but also potentially life-altering and even fatal medical conditions. According to a study in the journal Diabetes Care, of the 29.1 million Americans who live with diabetes, 15 percent will eventually develop ulcers. Eighty-four percent of all lower-limb amputations are preceded by ulcers. Clinicians are continually exploring new ways to combat this condition better. A combination of surgical and antibiotic treatment is mandatory in virtually all wound infections [11]. Local drug delivery can attain a concentration of more than a hundredfold higher for the drugs in surgical grafting or infection sites compared to a systemic drug regimen [12]. GSH, in addition to being the most potent antioxidant, is also a powerful anti-inflammatory agent [13]. Immobilizing glutathione with a skin graft or bandage via a nanofiber mesh can maintain skin regeneration and control microbial-induced inflammation [14]. Drugs can also be released at the implant site long enough to maintain the proper tissue function around the implant without causing any side effects [15]. We have developed an electrospun nanofiber membrane NFM that can be used as a drug delivery system. The goal of this study was to develop a method to attach GSH with PCL NFM and determine whether the produced fiber mesh can be used as a transdermal anti-oxidative drug delivery system. The mechanism of attaching nanofiber with drugs (infection resistant) will prevent the growth of bacteria. GSH, a powerful antioxidant naturally produced in the body, is a small tripeptide molecule composed of three amino acids: glutamic acid, cysteine, and glycine. The antioxidant activity of GSH is well established in various research. GLU is a clear liquid that is primarily used for the sterilization of medical equipment. It has a highly reactive chemical characteristic and antibacterial activity. The attachment of drugs (GSH-GLU) to the PCL nanofiber is a mechanism that this study is pursuing in which the drug would release gradually and steadily. This also is considered the novelty of our study by having a skin equivalent or wound healing model for diabetic patients that not only targets the antibacterial properties but the antioxidant purposes. The released GSH will prevent inflammation and any other undesired effect that might lead to the progression of the disease or in worst cases, surgeries such as amputation. This, in turn, would not only be cost-effective but also reduce the healing time of wounds.

2. Materials and Methods

2.1. Materials

This study used poly (ε-caprolactone) beads (pellet size~3 mm, average Mn 80,000) and acetone (laboratory reagent $\geq$ 99.5%) to prepare the PCL fibers. The set up is shown in

Figure 1a which demonstrates the whole unit including the syringe pump, electrical source, and collecting wire. Figure 1b shows the needle with attached high voltage current and the parallel collecting wires. This study used reduced glutathione and glutaraldehyde with 0.0055 g/mL concentration in PBS and GLU solution in order to produce the GSH solution and immobilization with PCL. Anti-glutathione antibody was used for the detection of GSH attachment with PCL NFM as described below. All chemicals were purchased from Sigma Aldrich. For bacterial analysis, this study used *Staphylococcus aureus* bacteria on TSA, TSB medium. Gentamicin (10 mg/mL), PCL, PCL-GSH, PCL-GLU were the sample groups.

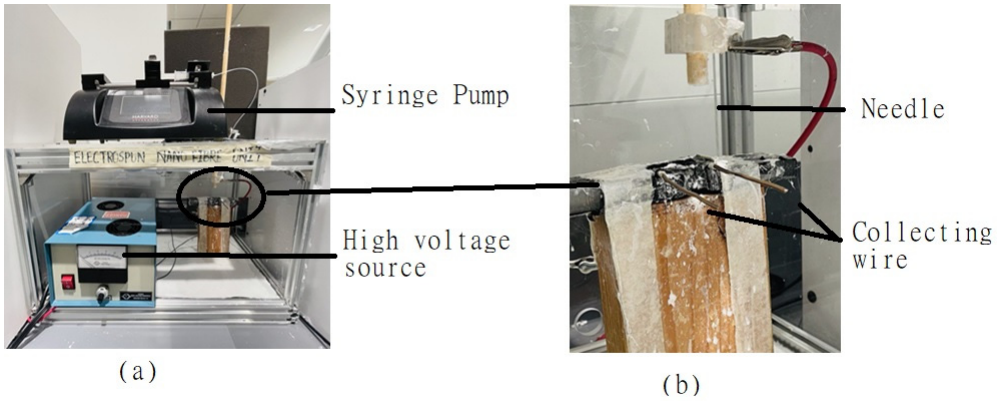

Figure 1. Electrospun nanofiber unit to produce PCL NFM. (**a**) Entire setup and (**b**) magnified inset from circled area in (**a**) showing nanofiber mesh collection setup consisting of two parallel rods.

2.2. Sample Preparation

This study produced PCL NFM using an electrospun process which was presented in our earlier publication [16]. In short, PCL beads and acetone were sonicated for 45 min, and then the solution was poured into a 12 mL plastic syringe. A syringe pump ejected the PCL solution through a metallic needle (23 G blunt needle, aluminum make, 25.4 mm length. Model # BX 25). The needle was charged with 9 kV of power. A PCL fiber layer was collected on two parallel wire ground collectors (Figures 1b and 2). A 10 mL cell culture plastic pipet was cut about 5 cm height each, and six layers of cross-direction PCL NFM were collected on one of the open ends of the tube through six repeated forward and backward motions (Figure 2, right image). The fiber was collected roughly at a right angle to the next layer to produce cross-directional PCL NFM.

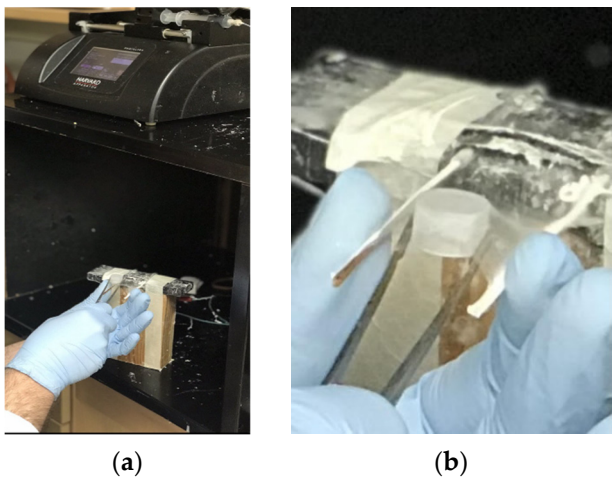

Figure 2. (**a**) Preparation of sample molds with nanofiber mesh in electrospun environment. (**b**) thin PCL film being collected onto a plastic cylinder.

This study produced three groups of samples (Figure 3). The collected PCL nanofibers on the tube were soaked with PBS overnight and then sterilized for 2 h under UV light to produce the PCL fibers. The sample was then left to air-dry and subsequently soaked for 48 h with glutathione and glutaraldehyde, or PBS-diluted glutathione solutions to produce two groups of GSH immobilized PCL fiber, referred to as PCL-GSH-PBS and PCL-GSH-GLU, respectively. Glutathione concentration in the GSH-PBS solution for each PCL NFM was 0.0055 g/mL. This value is equivalent to the dosage used daily on mice for our in vivo studies.

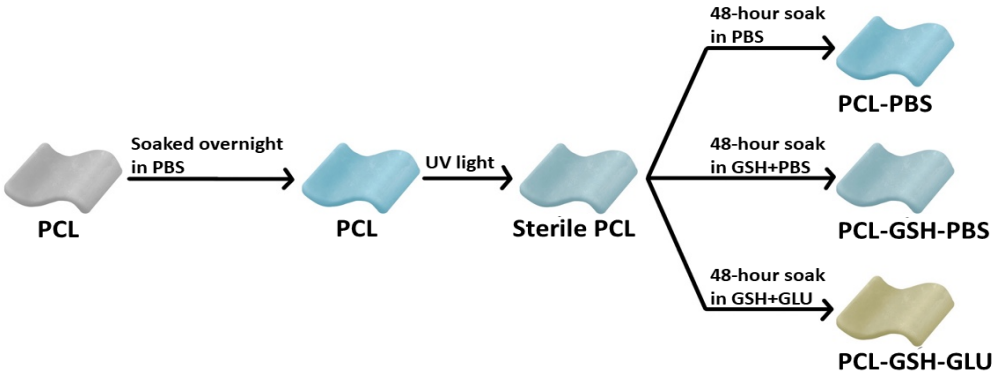

Figure 3. Schematic representation of study sample preparation.

2.3. PCL NFM Degradation

The surface morphology of PCL NFM was evaluated with a scanning electron microscope (Hitachi S-4800 Field Emission Scanning Electron Microscope (SEM) with EDS). The fiber mesh surfaces were coated with a thin layer of gold/palladium (Au/Pd) alloy before SEM imaging. The SEM images were obtained with maximal resolution up to 150 eV at an accelerating voltage of 10 kV and magnification up to 10,000×. This study used Image J software to measure the range of fiber diameters (AFD) from the captured SEM images.

Each tube holding the nanofibers was placed in a cell culture well filled with PBS solution where the fiber side of the tube was placed at the bottom of the well. The weight of the tube with fiber was the initial weight, W_o. Samples were washed daily and placed in a fresh PBS solution. Samples were air-dried and the weight was measured at 10- and 20-day intervals. We air-dried each sample using a mild speed air blower to remove any loose degraded particles and measured the dry weight, W_d. Each sample was returned to a freshly filled PBS well. The weight loss (degradation) at each time interval was calculated in percentage by the following equations.

$$\frac{(W_d - W_0)}{W_0} \times 100\%$$

2.4. GSH Adhesion and Release Assays

Two assays were conducted to determine: 1. whether GSH could bind to PCL nanofibers; and 2. whether the bound GSH could persist over time. To determine the ability of GSH to adhere to PCL nanofibers, samples were stained using indirect immunofluorescence. Samples were fixed using 4% paraformaldehyde, permeabilized with 0.1% Triton-X-100, then incubated for 1 h at room temperature in rabbit polyclonal anti-glutathione primary antibody (Sigma AB5010, CHEMICON, Darmstadt, Germany 1:100 dilution), washed, then secondarily labeled using goat anti-rabbit Alexa 488 (Invitrogen; Thermo Fisher, Waltham, MA, USA, 1:200 dilution). Samples were mounted with 80% glycerol/PBS and photographed using an Olympus IX-71 fluorescence microscope with DP72 camera and CelSens software (Olympus).

To determine the robustness of GSH attachment, GSH releasing tests were conducted on PCL-GSH-PBS and PCL-GSH-GLU for four-time intervals (1 h, 1 day, 10 days, and 20 days). The fiber sheets from the degradation tests were collected after 1 h, 1 day, 10 days,

and 20 days for the glutathione detection with different groups of nanofiber meshes. Additionally, the supernatants from the degradation tests were collected after 1 h, 1 day, 10 days, and 20 days for the GSH release test. These days were selected to determine initial GSH release and based on the same time intervals used in the in vivo study [17] to examine whether there was a release of GSH in PBS solution for 10 and 20 days intervals. This study followed the instructions of the (Invitrogen) Glutathione Colorimetric Detection Kit (cat.no. EIAGSHC) to measure the amount of GSH released from the supernatants.

2.5. Cell Proliferation Assay

For all experiments requiring cell culture, rat fibroblasts were cultured in a 5% CO_2 incubator at 37 °C, in media composed of DMEM (GIBCO/Invitrogen) + 5% fetal bovine serum. Single layers of aligned uni-directional PCL, PCL-GSH-PBS, and PCL-GSH-GLU nanofibers were incubated for 24 h with fibroblasts in media to measure the cell proliferation. Proliferation was studied using a label-ready ethynyl deoxyuridine (EdU) nucleotide followed by click chemistry using a kit (Click-iT; Invitrogen, Thermo Fisher, Waltham, MA, USA) as per manufacturer's instructions. Pre-cultured fibroblasts were mixed with medium and then seeded in a 96-well plate at 1×10^3 cells per well, then left for two days to incubate. On the second day, EdU diluted in a half volume of fresh media was added to each well at a final concentration of 10 micromolar. Cells were incubated in culture conditions for 24 h in the presence of EdU so that proliferating cells could incorporate it into replicating DNA. After continued incubation for 24 h, the cells were fixed with 4% paraformaldehyde for 20 min. After 3 PBS washes, 0.05 M of Tris buffer was added to the samples and left for 30 min to quench residual aldehydes. Click-chemistry staining of the EdU nucleotide was conducted for 30 min, followed by washes and mounting in 80% glycerol/PBS. Images were obtained using an Olympus IX-71 inverted fluorescent microscope using an Olympus DP72 camera, and captured using CelSens software (Olympus).

2.6. Cell MTT Assay

Cells were plated onto the samples including control (cells in media without treatments) and left in the incubator for 2 days. On the second day, the Vybrant MTT Cell Proliferation Assay Kit (Thermo Fisher, Waltham, MA, USA) was used to conduct MTT assay. The assay measures a cell's ability to metabolize MTT, which is linearly correlated to cell number. 12 mM MTT stock solution was made by mixing 1 mL of PBS into the vial labeled (MTT 3-(4,5-dimethylthiazol-2-yl)-2,5-diphenyltetrazolium bromide, component A) that was provided by the kit. 10 mL of Acetic acid was added into a tube containing SDS sodium dodecyl sulfate (component B) to completely dissolve the SDS powder. Once the solutions were made, media was completely aspirated from the samples and replaced with 100 microliters of fresh media. 10 microliters of component A were added into each well and left to incubate for 4 h. After 4 h, 100 microliters of component B were added to each well and mixed thoroughly using a pipette (10 microliters of the MTT stock solution for the negative control was also added to 100 microliters of medium alone). This was left for an additional 4 h in the incubator. The samples were then mixed and placed in a microplate reader (BioTek Synergy H1; Agilent Technologies, Santa Clara, CA, USA) and read at an absorbance of 540 nm. The results were then tabulated and made into graphs.

2.7. LDH Cytotoxicity Assay

A cytotoxicity test was conducted on the cells cultured overnight in the three tested conditions following the protocol of the CyQUANT™ LDH Cytotoxicity Assay Kit (C20301) used as directed. The kit measured lactate dehydrogenase released from the cells into the media surrounding cells, which is an indicator of cellular cytotoxicity. To determine the effectiveness of the assay to measure a positive response, 1X LDH Positive Control was made by diluting 1.5 µL of LDH Positive Control with 1 mL of 1% BSA in PBS. One batch of serial dilutions was lysed and used to measure the Maximum LDH Release. The second round of serial dilutions was used to determine the Spontaneous LDH release. The cells

were then incubated in a 37 °C incubator overnight. To the Spontaneous LDH Release dilution series of triplicate wells containing cells, 10 µL of sterile water was added. The Maximum LDH Release dilution series was increased by 10 µL of 10X Lysis buffer. After 45 min in an incubator at 37 °C, 50 µL of each sample medium was transferred to a 96-well flat-bottom plate in triplicate wells. Each sample's wells received 50 µL of Reaction Mixture. After incubating the plate for 30 min, 50 µL of Stop Solution was added to each sample well. Within 1 to 2 h of adding Stop Solution, the absorbance was measured at 490 and 680 nanometers. The absorbance value from 680 nm was subtracted from the 490 nm absorbance value to determine the LDH activity.

2.8. Antibacterial Analysis

PCL disks were exposed to UV light about 3 to 6 h prior to sample preparation. PCL-GSH-GLU and PCL-GSH-PBS were prepared a day before the experiment. PCL-GLU discs were prepared alongside the other sample groups to ensure the activity of GLU. PCL mesh circles were formed using a 9 mm puncher followed by placing 10 µL gentamicin on one PCL disc. The spreader was sterilized with ethanol and flaming sterilization. 100 µL of *Staphylococcus aureus* (ATCC 25923) was spread evenly throughout the tryptic soy agar plate. Discs (treated sample groups, positive control-gentamicin and negative control PCL) were gently placed on the agar plate containing the bacteria under aseptic conditions. After 20 h of incubation at 37 °C, antibacterial activity was evaluated by measuring the diameter of the clear zone; the average diameter of the inhibition zone surrounding the disk was measured with the help of a ruler. The mean reported for each sample group was based on three replicates.

2.9. Statistical Analysis

The KaleidaGraph software statistical analysis tool was used to differentiate factors (group) in the study parameters [15]. Independent sample *t*-tests were used to test for differences in mean cell proliferation and adhesion, degradation and releasing, cytotoxcicity, MTT assay, bacterial analysis and the variation between the control and treated samples. Differences between the two groups were determined one-way ANOVA with values of $p < 0.05$ considered statistically significant.

3. Results

3.1. GSH Attachment with Fiber Mesh

3.1.1. Morphology

Using the electrospinning process techniques that were demonstrated in Figure 2, PCL fibers were successfully collected onto the upper surface of each polystyrene cylinder (Figure 4a, left). At higher magnification the fiber orientation direction could be seen (Figure 4a, right); however, this magnification was too low to effectively measure the PCL fiber diameter. Therefore, SEM images were taken at 800× magnification (Figure 4b) for this purpose. Image J calculation found that fiber diameter in the mesh varied from 310 nm to 500 nm.

3.1.2. Degradation Analysis

There was no degradation of any sample group after 10 days; rather there was an increase of weight due to the absorption of GSH molecules (Table 1). There is no significant weight difference of any group of fiber mesh from 10 to 20 days. Additionally, GSH immobilization with PCL samples using either PBS or glutaraldehyde solution had no effect on absorption due to the perfect immobilization of GSH with PCL and its attachment to PCL.

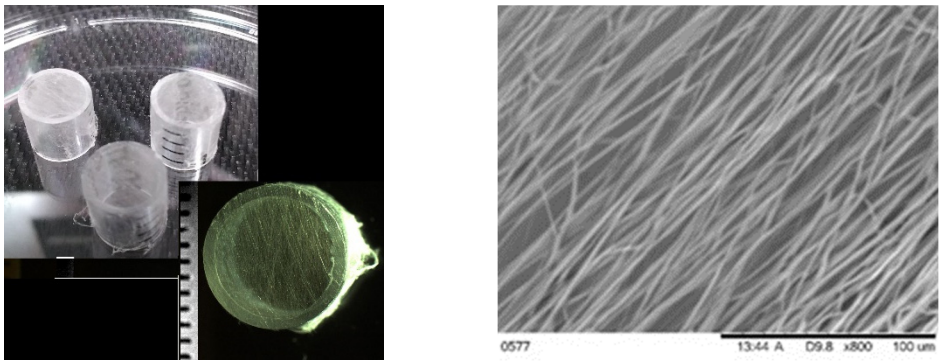

(**a**) (**b**)

Figure 4. (**a**) Produced PCL fiber membrane on a tube collector. The inset picture shows the PCL fiber mesh completely covered the hole of the tube; tick marks are 1 mm apart. (**b**) SEM image of an arbitrarily selected PCL fiber membrane from the produced samples before immobilization with GSH.

Table 1. Percentage of weight change of different sample groups after 10 and 20 days in soaking PBS (n = 5).

Sample Group	After 10 Days	After 20 Days
PCL-PBS	0.19 ± 0.08	0.21 ± 0.07
PCL-GSH-PBS	0.54 ± 0.05	0.54 ± 0.03
PCL-GSH-GLU	0.50 ± 0.04	0.50 ± 0.01

3.2. GSH Adhesion and Release Assays

Figure 5 shows the immunofluorescent identification of GSH adhesion to the nanofiber mesh. A homogenous attachment of GSH was observed from the fluorescent stained image. The green color indicated the presence of the secondary antibody (goat-anti-rabbit Alexa 488) bound to the primary GSH antibody.

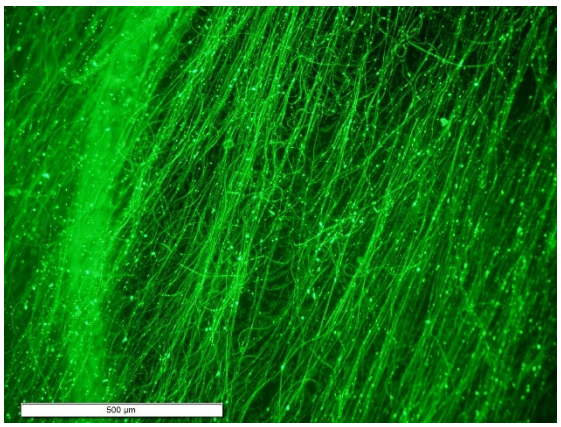

Figure 5. Anti-GSH antibody staining demonstrated the attachment of GSH to the PCL nanofibers. The value in the scale bar is 500 µm.

As seen in Figure 6, both GSH-immobilized samples released GSH for up to 20 days, although the GSH release rate was different. There was a large initial release of GSH (within an hour) from PCL-GSH-PBS samples. In contrast, the initial release of GSH from PCL-GSH-GLU samples was low. Within 24 h, the amount of GSH release from PCL-GSH-GLU samples was significantly lower compared to GSH release from PCL-GSH-PBS samples.

There was a steady amount of GSH release from both PCL-GSH-PBS samples after 24 h (n = 5).

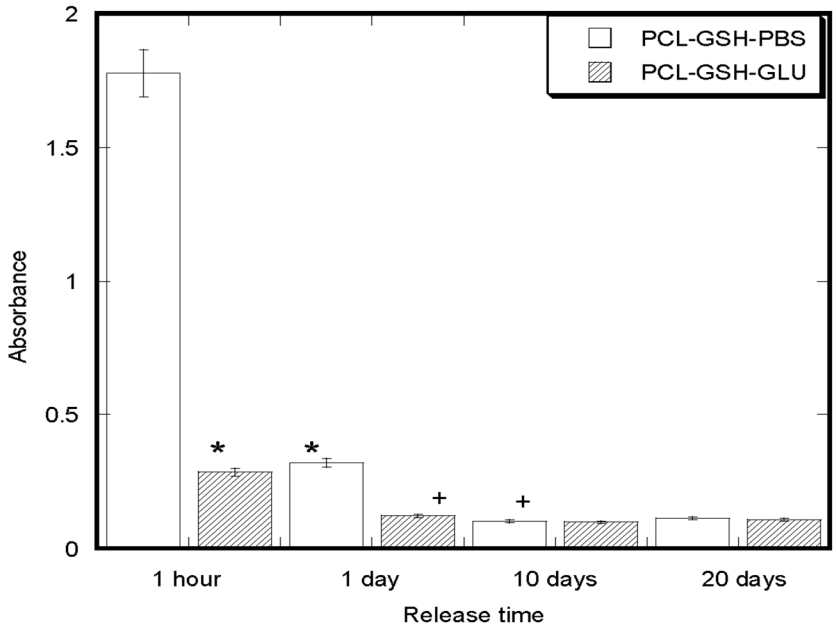

Figure 6. Glutathione release from PCL nanofibers during tested periods. In the figure, * refers $p < 0.05$ compared to PCL-GSH-PBS absorbance value after 1 h and * refers $p < 0.05$ compared to PCL-GSH-PBS absorbance value after 1 day. + refers $p < 0.05$ compared to PCL-GSH-PBS absorbance value after 10 days.

3.3. Cell Proliferation Assay

Figure 7a shows the cell proliferation on the control group (PCL only) where those green dots are representing the labeled nuclei and the fiber structure is the PCL that cells are rest on, and Figure 7b illustrates the cell viability on PCL-GSH-GLU where the green dots represent the cells on fiber structure and showing the highest proliferation sample group. Lastly Figure 7c demonstrates the proliferation of PCL-GSH-PBS where the green dots are representing the cells on fiber structure. The presence of green circles indicates nuclei of proliferating cells. (n = 4).

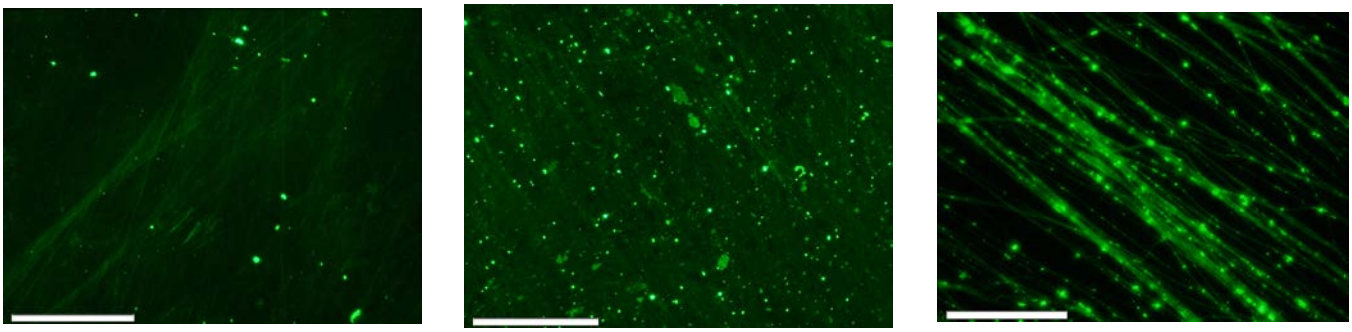

(a) (b) (c)

Figure 7. Cell proliferation as demonstrated by labeled nuclei of (**a**) PCL (Control), (**b**) PCL-GSH-GLU and (**c**) PCL-GSH-PBS. The value in the scale bar is 500 μm.

3.4. Cell MTT Assay

Cells in all treatments were able to metabolize MTT as shown by absorbance measurement. All samples including the control (cells in media without treatments) metabolized MTT to a similar degree (Figure 8). There was no statistically significant difference of cell viability observed among the sample groups.

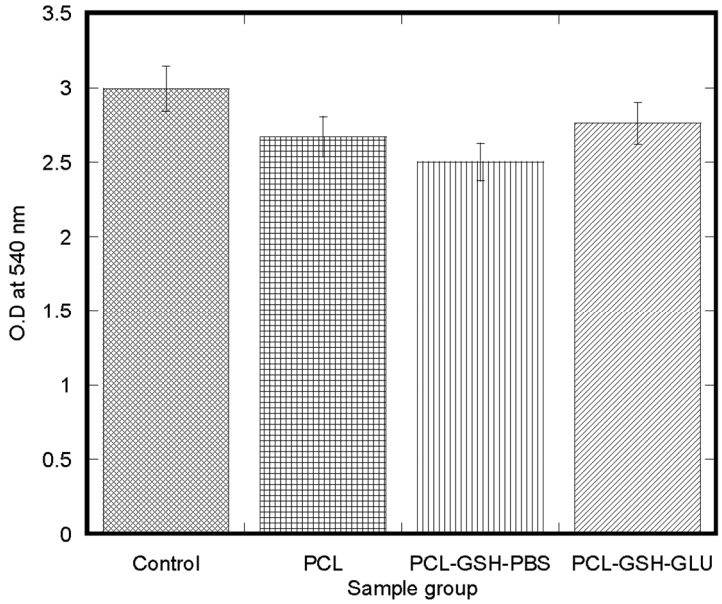

Figure 8. Analyses of MTT metabolic activity by fibroblasts cultured in tested conditions (n = 4). No statistical significant differences were found between any group in the figure.

3.5. Cytotoxicity Assay

Absorbance of LDH present in media was measured to determine cytotoxicity (Figure 9). High absorbance of LDH in media not exposed to cells (control, left bar) indicated the assay was able to detect cytotoxicity. All samples showed reduced absorbance relative to control (Figure 9). Among the sample groups the PCL-GSH-GLU shows the lowest absorbance of 0.027. PCL-GSH-PBS and PCL groups show the absorbance of 0.296 and 0.171 respectively.

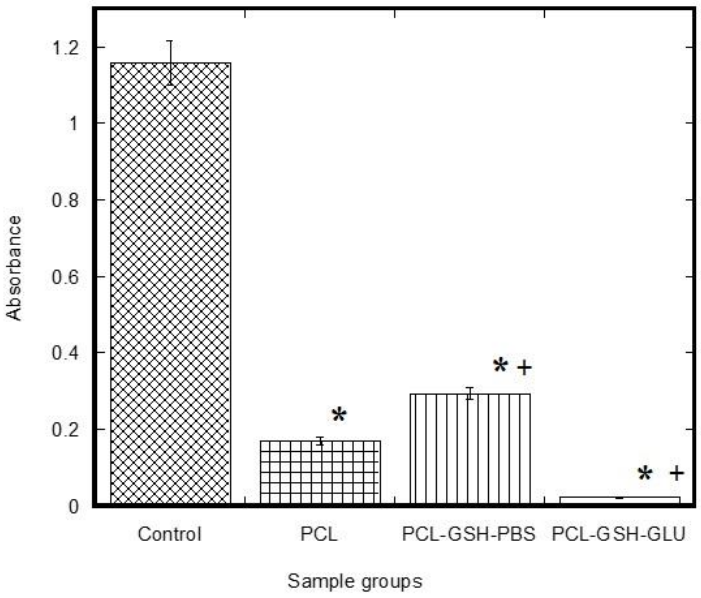

Figure 9. Cytotoxicity test result for PCL-GSH-GLU, PCL-GSH-PBS, PCL only and control (n = 4). In the figure, In the figure, * refers $p < 0.05$ compared to control Absorbance of LDH value and + refers $p < 0.05$ compared to PCL Absorbance of LDH value.

3.6. Bacterial Evaluation of GSH and GLU

The Kirby-Bauer Disk Diffusion/Inhibition Test was conducted and as Figure 10 shows the results confirmed the antibacterial properties of GLU and PCL-GSH-GLU. Based on Figure 10a the inhibition zone of 12.5 mm is depicted which confirms the antibacterial

properties of GLU. Figure 10b shows the inhibition zone of 13 mm for PCL-GSH-GLU. Figure 10c confirmed the inactivity of antibacterial properties of GSH as demonstrated in the inhibition zone of zero in the PCL-GSH-PBS group. Figure 10d,e illustrate the positive (gentamicin) and negative (only PCL) control with an inhibition zone of 17 mm and zero respectively (Table 2).

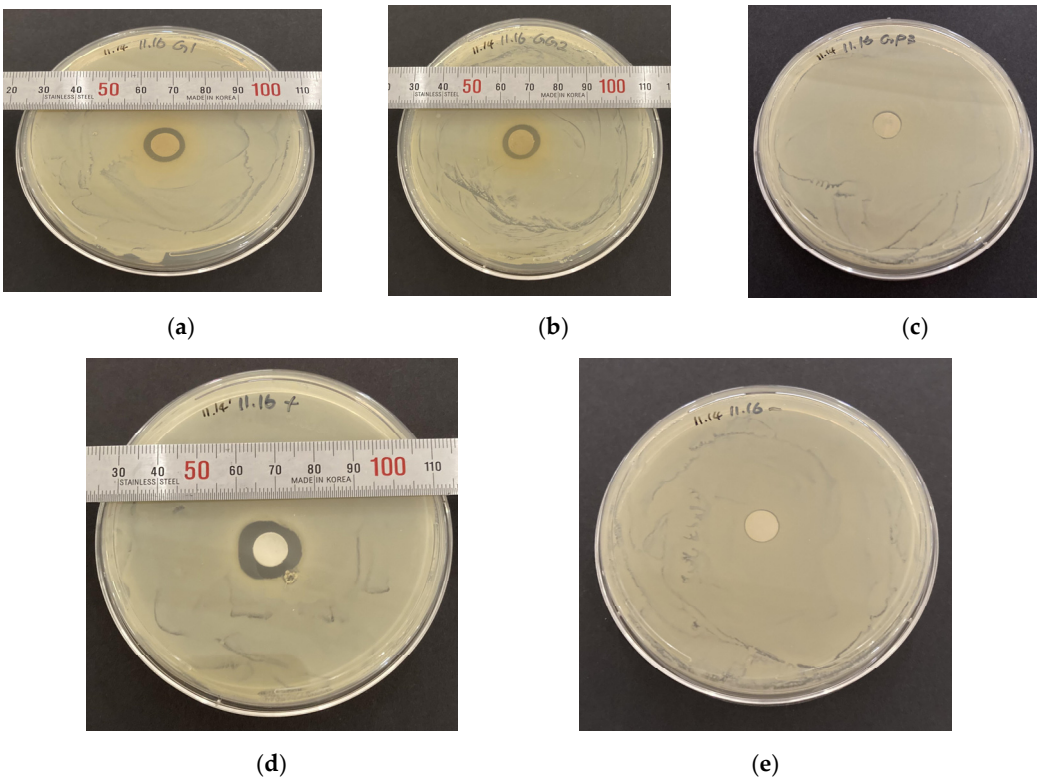

Figure 10. The result pictures of inhibition zone measurement for Kirby-Bauer Disk Diffusion/Inhibition Test. (**a**) PCL-GLU. (**b**) PCL-GSH-GLU. (**c**) PCL-GSH-PBS. (**d**) Positive control: Gentamicin. (**e**) Negative control: PCL.

Table 2. The diameter of the clear zone from the Kirby-Bauer Disk Diffusion method (n = 3).

	Inhibition Zone 1 (mm)	Inhibition Zone 2 (mm)	Inhibition Zone 3 (mm)	Inhibition Zone Average (mm)
PCL-GLU (G)	12.5	13.0	12.5	12.7
PCL-GSH-GLU (GG)	13.0	13.0	13.0	13.0
PCL-GSH-PBS (GP)	0	0	0	0
Positive Control (gentamicin)	17.0	-	-	17.0
Negative Control (only PCL)	0	-	-	0

4. Discussion

ROS are emerging as substances that cause several degenerative diseases such as diabetes [18]. ROS exists in various molecular forms such as H_2O_2, ions such as ClO-, superoxide anions, and free radicals such as ·OH. Superoxide anions in the body are produced during direct oxygen reduction when electrons leak from the electron transfer

chain and oxidative phosphorylation processes in mitochondria [19]. Since very unstable superoxide anions are converted to the more stable H_2O_2 by superoxide dismutase, most of the ROS observed in the body takes the form of H_2O_2. Most H_2O_2 is converted to non-toxic H_2O by antioxidants such as catalase and peroxidase in cells [20]. As described above, mitochondria are places where ROS are mainly produced, and the genome of mitochondria is vulnerable to oxidative damage and mutations caused by free radicals [21]. This is because the production of free radicals occurs nearby, and due to the nature of mtDNA, there are no histone proteins to protect and there is proofreading deficiency in mitochondrial DNA polymerase [22,23]. In particular, when fat accumulates in the body, overall oxidative stress increases due to an increase in NADPH oxidase, an enzyme that produces ROS in adipose cells, and a decrease in antioxidants [24]. These oxidative stresses cause various diabetes complications. In our earlier study, we found that the high levels of sugar in diabetic male mice were significantly decreased due to the daily injection of glutathione. Moreover, oxidative stress in diabetic male mice leads to depletion of total glutathione levels in body organs (pancreas, spleen, epididymis, and testis). Continuous exposure to antioxidants has been suggested as a treatment for alleviating diabetes complications and preventing diabetes from progressing [25]. We developed a nanofiber NFM containing drugs as a drug delivery method in this experiment.

GSH is an antioxidant found in animals, plants, and fungi which can be used as a substance that effectively neutralizes ROSs that have increased due to diabetes. GSH is a tripeptide protein that consists of three amino acids; glycine, glutamate, and cysteine [26]. The thiol group in cysteine reduces ROS, glutamate acts as an excitatory neurotransmitter, and glycine acts as an inhibitory neurotransmitter in the central nervous system. GSH makes oxidized vitamin C into reduced vitamin C that can pass through red blood cells and the blood-brain barrier (BBB). Vitamin C, upon entering red blood cells or BBB, is reduced again with the help of glutathione and is involved in the production and regulation of various neurotransmitters and hormones. In other words, GSH is the helper needed for vitamin C to work as a powerful antioxidant. GSH is synthesized 70% in the liver, 15% in the kidneys, and 15% in the lungs to protect all cells, tissues, and organs from ROS and diseases and to play a role in keeping the antioxidant network constant in the body [27]. In addition, GSH is a good anti-inflammatory substance by strengthening interleukin-1, which acts as an anti-inflammatory agent, and interleukin-2, which promotes immune cell differentiation and growth [25,28]. GLU is a disinfectant approved by the Centers for Disease Control and Prevention (CDC) mainly used to sterilize medical devices in hospitals and has sterilization and disinfection effects [29]. GLU deprotonates amines on the cell surface, therefore the structure of proteins is disrupted [30]. GSH is a water-soluble compound and GLU is a polar liquid, and miscible to water [26]. GLU has an antibacterial effect and not only acts as a good solvent to GSH but also shows better cell viability when the GSH-GLU combination is used.

Recent findings suggest the possibility of a new transdermal anti-oxidative drug delivery method based on the slow degrading rate of PCL. Several studies have been conducted for similar antibacterial purposes of releasing GLU using other polymer materials like polyurethane, yet the activity of glutaraldehyde was not sustained over long periods of time [31]. The property of PCL as being a synthetic biodegradable and bioresorbable polymer to be a proper biocompatible product, allows us to get benefit in several biomedical applications that have been approved by the FDA. PCL is a member of the aliphatic polyester family of compounds, whereby increasing the molecular weight its crystallinity would decrease. In addition, PCL has high crystallinity and hydrophobicity which makes this polymer degrade at a slow rate [32]. Based on our findings, no degradation on any sample group was seen after 10 days of incubation, but instead, the sample group demonstrated gaining weight. The degradation test showed increased weight in both GSH samples relative to PCL (control). This means that the hydrophilic characteristics of PCL can be improved by attaching GSH with PCL using GSH-PBS and GSH-GLU solutions. These results also suggested that the GSH attached with the PCL surface and increased the matrix

weight. Most importantly, the structural integrity of the fiber matrix was intact due to the GSH immobilization for up to 20 days. This also suggests that immobilizing GSH with PCL using glutaraldehyde solution, instead of PBS solution, stops the release of GSH from the nanofibers. This study also proposed that PCL-GSH-GLU samples could release GSH at a steady rate until the degradation of fiber. Since this study was limited to a 20 days' time interval and there was no observed degradation within 20 days, we are unable to test this proposition. Furthermore, this study found that when we immobilize the glutathione onto the PCL using PBS or GLU, glutathione was stuck to the PCL surface and immobilized evenly throughout the whole surface of the nanofibers (Figure 5).

Fibroblasts' ability to attach, metabolize and proliferate were demonstrated in two separate assays, EdU-click and MTT assays. MTT assay results showed the quantitative difference of cell attachment among the sample groups (Figure 8). While the average values of fibroblast metabolic activity in PCL and GSH immobilized PCL samples were lower than control, the differences were not statistically significant. The difference of O.D values between PCL and GSH-immobilized PCL surfaces was also insignificant. These findings indicate that the GSH-immobilized PCL nanofibers did not exert additional effects on cellular metabolism, and indirectly suggest adhesion was unaffected. Cells survived, adhered to, and proliferated on the PCL and GSH-immobilized PCL surfaces (Figure 7). A previous study [33] demonstrated when cells successfully bind to PCL they subsequently secrete extracellular matrix (ECM) to keep their surroundings suitable for growth. This cellular metabolic activity was slightly different from control (cells only in the well), where cells were homogeneously distributed around the well. Cell attachment similar to control can be achieved by using cross or random directions on multiple layers of fiber which was observed in our earlier study using mouse osteoblast cells [16].

The uniqueness of this study proposed that the dermal equivalent model -PCL collagen based [34] provides a suitable condition to have antibacterial properties as well as drug-releasing (GSH) properties. According to the degradation test, it was not showing any degradation after 10 days in any treated samples. However, the increase in weight was noticed in sample groups and that suggested PCL absorbed GSH and GLU. According to Table 1, there was a weight increase between PCL-PBS 0.19 and two other sample groups, PCL-GSH-PBS and PCL-GSH-GLU, of 0.54 and 0.50, respectively, after 10 days. This would confirm that GSH was absorbed into the PCL. On the other hand, based on the releasing test results, PCL-GSH-PBS and PCL-GSH-GLU both confirmed the release of GSH. The release of GSH in PCL-GSH-GLU was steady and gradually in which, referring to Table 1, the weight differences between these two sample groups with day 10 and 20 support this manner.

One appropriate indicator of cytotoxicity is release of cytosolic LDH through a damaged plasma membrane. LDH is a cytosolic enzyme that is present in many cells. The released LDH enters the cell culture medium and its enzymatic activity is measured; the activity is dependent on cell number. This suggests higher cell concentrations would demonstrate higher cytotoxicity. The obtained results highly demonstrated the low cell concentration or low toxicity of the treated sample groups compared to the control group. Yet among the sample groups, PCL-GSH-GLU demonstrated the lowest absorbance and cell concentration which, combined, demonstrated least toxicity (Figure 9). PCL and PCL-GSH-PBS groups show the next higher toxication respectively.

Antibacterial analysis revealed that GLU has antibacterial properties while GSH did not show any inhibition zone. According to Table 2, PCL-GLU shows the average of 12.7 mm inhibition zone and 13 mm for PCL-GSH-GLU respectively. This indicates that GLU itself has antibacterial properties and combining that with GSH demonstrated larger inhibition zones and ultimately stronger antibacterial products. The lack of a clear zone using PCL-GSH-PBS treatment (Figure 10c) suggests that GSH itself does not have the characteristics as an antibacterial drug.

Our finding suggests the application of GSH-GLU with the PCL fiber to increase the capability of anti-inflammatory and antibacterial properties of the product to be used

in several biomedical applications. However, it requires further study to expand the knowledge and findings to better understand the characteristics of GLU and GSH combined with PCL by conducting genome-based tests that include several methods to be able to characterize the bacterial activity interacting with these drugs. In addition, future work will be conducted with larger sample groups for better accuracy in results.

The translation of this study is to develop the skin equivalent model to add GSH combining with GLU and PBS to see the effect whether it has the antibacterial and drug releasing properties. In our previous study we already developed a collagen PCL based skin equivalent model [34]. In that research study we found that PCL collagen is a suitable model for skin equivalent. In this paper we tried to add GSH with different solvent of GLU and PBS to see the outcome of the skin model in order to find a suitable model for diabetic patients. As part of our limitation in this study, we considered the in vitro study over the treated skin equivalent model. In our separate ongoing research, we are currently doing animal study with the PCL collagen based skin model which the result is going to publish in a separate paper.

5. Conclusions

This study targets the unique idea of attaching electrospun PCL nanofiber mesh to anti-oxidative and anti-inflammatory drugs such as GSH and GLU. The present investigation found that GSH attachment to PCL nanofiber is possible by soaking PCL fiber with a GLU solution. The results suggest that PCL-GSH-GLU fiber mesh is biocompatible and may provide the fiber mesh antioxidation characteristics of GSH and antibacterial characteristics of GLU. The fiber mesh has adequate degradation and cell viability characteristics. In addition, the fiber mesh can release GSH for a prolonged period. Therefore, this study results confirmed the advantage of using PCL combined with GSH and GLU that can be used as a transdermal anti-oxidative and antibacterial drug delivery system such as bandage, skin graft for wound healing application in a diabetic patient.

Author Contributions: M.K. imagined and formulated the experiments; H.K. and M.B.V. supervised and shared resources for the project. N.A. executed the morphological and cell experiments; H.P. produced the samples for the project; S.N. and J.J. performed the microbial analysis. M.K. created the plots based on the provided data and wrote the manuscript. N.A., S.N. and J.J. provided protocol and outcomes of the projects in written format for the manuscript. M.K., S.N., J.J. and M.B.V. edited and proofread the manuscript. All authors have read and agreed to the published version of the manuscript.

Funding: This research is supported by the National Institute of General Medical Sciences of the National Institutes of Health under award number 5P20GM103447, Office of Research and Sponsored programs. This research also supported by the University of Central Oklahoma on-campus grant, the College of Mathematics and Science CURE-STEM program and the STLR (Students' Transformative Learning Record).

Institutional Review Board Statement: Not applicable.

Informed Consent Statement: Not applicable.

Data Availability Statement: Essential data are contained within the article. The raw data are available on request from the corresponding author.

Acknowledgments: NIH Grant Number 5P20GM103447 support was used for this study. University of Central Oklahoma on-campus faculty grant and CURE-STEM awards was used for the publication.

Conflicts of Interest: The authors have no conflict of interest.

References

1. Maritim, A.C.; Sanders, R.A.; Watkins, J.B. Diabetes, oxidative stress, and antioxidants: A review. *J. Biochem. Mol. Toxicol.* **2003**, *17*, 24–38. [CrossRef] [PubMed]
2. Sekhar, R.V.; McKay, S.V.; Patel, S.G.; Guthikonda, A.P.; Reddy, V.T.; Balasubramanyam, A.; Jahoor, F. Glutathione Synthesis Is Diminished in Patients With Uncontrolled Diabetes and Restored by Dietary Supplementation With Cysteine and Glycine. *Diabetes Care* **2011**, *34*, 162–167. [CrossRef] [PubMed]
3. Bauche, F.; Fouchard, M.H.; Jegou, B. Antioxidant system in rat testicular cells. *FEBS Lett.* **1994**, *349*, 392–396. [CrossRef]
4. Matough, F.A.; Budin, S.B.; Hamid, Z.A.; Alwahaibi, N.; Mohamed, J. The role of oxidative stress and antioxidants in diabetic complications. *Sultan Qaboos Univ. Med. J.* **2012**, *12*, 5–18. [CrossRef] [PubMed]
5. Asmat, U.; Abad, K.; Ismail, K. Diabetes mellitus and oxidative stress—A concise review. *Saudi Pharm. J.* **2016**, *24*, 547–553. [CrossRef] [PubMed]
6. Vega-Lopez, S.; Devaraj, S.; Jialal, I. Oxidative stress and antioxidant supplementation in the management of diabetic cardiovascular disease. *J. Investig. Med. Off. Publ. Am. Fed. Clin. Res.* **2004**, *52*, 24–32.
7. Dreher, I.; Schütze, N.; Baur, A.; Hesse, K.; Schneider, D.; Köhrle, J.; Jakob, F. Selenoproteins are expressed in fetal human osteoblast-like cells. *Biochem. Biophys. Res. Commun.* **1998**, *245*, 101–107. [CrossRef]
8. Thrailkill, K.M.; Lumpkin, C.K.; Bunn, R.C.; Kemp, S.F.; Fowlkes, J.L. Is insulin an anabolic agent in bone? Dissecting the diabetic bone for clues. *Am. J. Physiol. Endocrinol. Metab.* **2005**, *289*, 735–745. [CrossRef]
9. Janghorbani, M.; Feskanich, D.; Willett, W.C.; Hu, F. Prospective study of diabetes and risk of hip fracture: The Nurses' Health Study. *Diabetes Care* **2006**, *29*, 1573–1578. [CrossRef]
10. Vig, K.; Chaudhari, A.; Tripathi, S.; Dixit, S.; Sahu, R.; Pillai, S.; Dennis, V.A.; Singh, S.R. Advances in Skin Regeneration Using Tissue Engineering. *Int. J. Mol. Sci.* **2017**, *18*, 789. [CrossRef]
11. Van Baal, J.G. Surgical Treatment of the Infected Diabetic Foot. *Clin. Infect. Dis.* **2004**, *39* (Suppl. S2), S123–S128. [CrossRef] [PubMed]
12. Gottumukkala, S.N.V.S.; Sudarshan, S.; Mantena, S.R. Comparative evaluation of the efficacy of two controlled release devices: Chlorhexidine chips and indigenous curcumin based collagen as local drug delivery systems. *Contemp. Clin. Dent.* **2014**, *5*, 175–181. [CrossRef] [PubMed]
13. Weschawalit, S.; Thongthip, S.; Phutrakool, P.; Asawanonda, P. Glutathione and its antiaging and antimelanogenic effects. *Clin. Cosmet. Investig. Dermatol.* **2017**, *10*, 147–153. [CrossRef] [PubMed]
14. Khandaker, M.; Riahinezhad, S.; Jamadagni, H.G.; Morris, T.L.; Coles, A.V.; Vaughan, M.B. Use of Polycaprolactone Electrospun Nanofibers as a Coating for Poly(methyl methacrylate) Bone Cement. *Nanomaterials* **2017**, *7*, 175. [CrossRef]
15. Sharma, S. Local Drug Delivery System. Available online: https://www.slideshare.net/sapna27sharma/local-drug-delivery-system (accessed on 23 January 2022).
16. Sultana, F.; Vaughan, M.; Khandaker, M. Effect of Fiber Architecture on the Cell Functions of Electrospun Fiber Membranes. In *Proceedings of the 2016 Annual Conference on Experimental and Applied Mechanics*; Springer International Publishing: Cham, Switzerland, 2017; Volume 6, pp. 157–160.
17. Al Kadhem, N.; Al Ani, N.; Pasini, M. Study theEffects of Glutathione (GSH) on Blood Glucose Level in Diabetic Male Mice. *Al-Nahrain J. Sci.* **2013**, *16*, 230–238. [CrossRef]
18. Lee, H.C.; Wei, Y.H. Mitochondrial role in life and death of the cell. *J. Biomed. Sci.* **2000**, *7*, 2–15. [CrossRef] [PubMed]
19. D'Autréaux, B.; Toledano, M.B. ROS as signalling molecules: Mech- anisms that generate specificity in ROS homeostasis. *Nat. Rev. Mol. Cell Biol.* **2007**, *8*, 813–824. [CrossRef] [PubMed]
20. Sheng, Y.; Abreu, I.A.; Cabelli, D.E.; Maroney, M.J.; Miller, A.F.; Teixeira, M.; Valentine, J.S. Superoxide Dismutases and Superoxide Reductases. *Chem. Rev.* **2014**, *114*, 3854–3918. [CrossRef]
21. Croteau, D.L.; Bohr, V.A. Repair of oxidative damage to nuclear and mitochondrial DNA in mammalian cells. *J. Biol. Chem.* **1997**, *272*, 25409–25412. [CrossRef]
22. Furukawa, S.; Fujita, T.; Shimabukuro, M.; Iwaki, M.; Yamada, Y.; Nakajima, Y.; Nakayama, O.; Makishima, M.; Matsuda, M.; Shimomura, I. Increased oxidative stress in obesity and its impact on metabolic syndrome. *J. Clin. Investig.* **2004**, *114*, 1752–1761. [CrossRef]
23. Bogenhagen, D.F. Mitochondrial DNA nucleoid structure. *Biochim. Biophys. Acta* **2012**, *1819*, 914–920. [CrossRef] [PubMed]
24. Liao, N.; Shi, Y.; Zhang, C.; Zheng, Y.; Wang, Y.; Zhao, B.; Zeng, Y.; Liu, X.; Liu, J. Antioxidants inhibit cell senescence and preserve stemness of adipose tissue-derived stem cells by reducing ROS generation during long-term in vitro expansion. *Stem Cell Res. Ther.* **2019**, *10*, 306. [CrossRef] [PubMed]
25. Nickovic, V.P.; Miric, D.; Kisic, B.; Kocic, H.; Stojanovic, M.; Buttice, S.; Kocic, G. Oxidative stress, NOx/l-arginine ratio and glutathione/glutathione S-transferase ratio as predictors of 'sterile inflammation' in patients with alcoholic cirrhosis and hepatorenal syndrome type II. *Ren. Fail.* **2018**, *40*, 340–349. [CrossRef]
26. Masella, R.; Mazza, G. *Glutathione and Sulfur Amino Acids in Human Health and Disease*, 1st ed.; Wiley: New York, NY, USA, 2009.
27. Zhang, Z.; Hao, H.; Wu, X.; Wang, Q.; Chen, M.; Feng, Z.; Chen, H. The functions of glutathione peroxidase in ROS homeostasis and fruiting body development in Hypsizygus marmoreus. *Appl. Microbiol. Biotechnol.* **2020**, *104*, 10555–10570. [CrossRef]

28. Peran, L.; Camuesco, D.; Comalada, M.; Nieto, A.; Concha, A.; Adrio, J.L.; Olivares, M.; Xaus, J.; Zarzuelo, A.; Galvez, J. Lactobacillus fermentum, a probiotic capable to release glutathione, prevents colonic inflammation in the TNBS model of rat colitis. *Int. J. Colorectal Dis.* **2006**, *21*, 737–746. [CrossRef]
29. Russell, A. Glutaraldehyde: Current Status and Uses. *Infect. Control Hosp. Epidemiol.* **1994**, *15*, 724–733. [CrossRef] [PubMed]
30. Bruck, C.W. Role of glutaraldehyde and other liquid chemical sterilants in the processing of new medical devices. In *Sterilization of Medical Products*; Polyscience Publications: Laval, QC, Canada, 1991; pp. 376–396.
31. Sehmi, S.K.; Allan, E.; MacRobert, A.J.; Parkin, I. The bactericidal activity of glutaraldehyde-impregnated polyurethane. *MicrobiologyOpen* **2016**, *5*, 891–897. [CrossRef] [PubMed]
32. Herrero-Herrero, M.; Gómez-Tejedor, J.; Vallés-Lluch, A. PLA/PCL electrospun membranes of tailored fibres diameter as drug delivery systems. *Eur. Polym. J.* **2018**, *99*, 445–455. [CrossRef]
33. Jhala, D.; Rather, H.; Kedaria, D.; Shah, J.; Singh, S.; Vasita, R. Biomimetic polycaprolactone-chitosan nanofibrous substrate influenced cell cycle and ECM secretion affect cellular uptake of nanoclusters. *Bioact. Mater.* **2019**, *4*, 79–86. [CrossRef]
34. Khandaker, M.; Nomhwange, H.; Progri, H.; Nikfarjam, S.; Vaughan, M.B. Evaluation of Polycaprolactone Electrospun Nanofiber-Composites for Artificial Skin Based on Dermal Fibroblast Culture. *Bioengineering* **2022**, *9*, 19. [CrossRef]